Development of a photosynthesis measurement chamber under different airspeeds for applications in future space crop-production facilities

Lucie Poulet[1]
NASA Postdoctoral Program, USRA, Kennedy Space Center, FL, 32899, USA

Michael K. Gildersleeve[2]
NIF/OSTEM Internship Program, Kennedy Space Center, FL, 32899, USA
Cornell University, NY, 13112, USA

Lawrence L. Koss[3]
Kennedy Space Center, Amentum Services, Inc., FL, 32899, USA

and

Gioia D. Massa[4], Raymond M. Wheeler[5]
NASA, Kennedy Space Center, FL, 32899, USA

Space crop production systems are being developed to grow fresh produce in-situ to supplement the astronauts' diet, but the required ventilation rates for crops in different gravity environments remains poorly understood. The reduction or lack of buoyancy-driven convection in reduced gravity environments leads to impaired gas exchange (CO_2 absorption, water transpiration and O_2 release) at the leaf surface if no extra ventilation is provided, and this could lead to a reduction in biomass production in the long run. To better characterize the influence of different airspeeds on photosynthesis and be able to model this in low gravity, a chamber was designed to interface with a LI-6800 portable photosynthesis system. This paper details the design of this chamber, specifically made to measure whole-plant and small canopy gas exchange at different airspeeds. The fans provide turbulent mixing in the chamber to ensure that it behaves like a continuous stirred tank reactor (CSTR) and that the residence time distribution (RTD) is the same for any fan speed; the computational fluid dynamic (CFD) model of the gas domain (the air in the chamber) hence uses a k-omega turbulence model. An airflow map of the chamber was created using anemometer measurements for the different airspeeds tested, and this was used together with the CFD simulation results to relate the experimentally measured fan outputs to actual airspeeds on top of an artificial plant. Environmental parameters (air temperature, relative humidity, CO_2 level) are controlled by the LI-6800. This work was funded by NASA Space Biology through the NASA postdoctoral program / USRA.

[1] NASA Postdoctoral Research Fellow, Exploration Research and Technology Programs, Mail Code: UB-A Kennedy Space Center, FL 32899 USA.
[2] NIF/OSTEM Intern, Exploration Research and Technology Programs, Mail Code: UB-A Kennedy Space Center, FL 32899 USA.
[3] Engineering Technician VI, Amentum Services, Mail Code: LASSO-008, Kennedy Space Center, FL 32899.
[4] Senior Scientist, Exploration Research and Technology Programs, Mail Code: UB-A, Kennedy Space Center, FL 32899 USA.
[5] Senior Scientist, Exploration Research and Technology Programs, Mail Code: UB-A, Kennedy Space Center, FL 32899 USA.

I. Introduction

LONG-duration space exploration missions will require astronauts to produce their food in-situ, in order to have a sustainable food supply. Plants can ensure functions such as food production, air revitalization, and water purification – this makes them of prime importance for a Lunar or a Martian settlement[1, 2, 3]. To rely on plants for life-support system functions, we need to understand their growth and development processes in reduced gravity.

A. Gas exchange in reduced gravity

In particular, the decrease or lack of buoyancy-driven convection in environments where gravity levels are below 1g has a negative impact on gas exchange (CO_2 absorption, water transpiration and O_2 release); this could translate into reduced biomass production[4, 5]. To address this, fans are added to plant growth hardware on the International Space Station (ISS)[6, 7, 8], but the minimal forced ventilation required for optimal photosynthesis in different gravity levels has not yet been quantified. This has two consequences on the design of future large-scale plant growth modules:

1- Fans could be a significant source of energy waste if not tailored to the particular plant species, age, and environment;
2- The food (and oxygen) production could be lower than expected. Indeed, it is not possible to achieve a homogeneous airflow everywhere in a large-scale crop production facility, so there will be crops growing under a suboptimal airflow, which could lead to a decreased yield[9].

B. Rationale of designing a custom-made measurement chamber

Characterizing the influence of different airspeeds on photosynthesis in reduced gravity environments can be achieved with a calibrated mechanistic model, coupling a mass and energy balance[10, 11]. Data acquisition in laboratory environments in 1g helps calibrate the model that can later be used for predictions in environments with lower gravity. Therefore, whole plant and small canopy gas exchange measurements are necessary.

The LI-6800 (LI-COR, Inc., Lincoln, NE) is an open system equipped with infrared gas analyzers (IRGA), which measure the difference of CO_2 and H_2O in the air entering and exiting the leaf / plant chamber. Based on a mass balance approach, relying on the hypothesis of a continuous stirred tank reactor (CSTR), it computes the CO_2 assimilation rate and transpiration rate of the leaf / plant.

In its standard configuration, the LI-6800 is a portable photosynthesis measurement instrument, enabling non-destructive measures of leaf-level photosynthesis processes. To make whole plant predictions, however, we need to calibrate the mechanistic model needs over a whole plant or a canopy. Therefore, we designed a plant chamber that interfaces with the LI-6800, enabling gas exchange measurements for different airspeeds, at the whole plant and small canopy level. An adapter (Figure 1) allows the interface between the custom-made chamber and the LI-6800 head. Hence, all environmental parameters within the chamber (air temperature and relative humidity, CO_2 level) are controlled by the LI-6800. To ensure that measurements are accurate, the hypothesis of stirred tank reactor must be verified in the custom chamber. This is achieved by analyzing the air residence time distribution (RTD) within the chamber, i.e. the time that air will stay in the chamber, for different ventilation configurations, as detailed in section II. This analysis led to the positioning of the fans, as well as the resulting airflow maps. Section III, details the computational fluid dynamics (CFD) performed on this chamber to better characterize the air velocities within it, especially at the leaf's surfaces, ensuring that they are low.

II. Design overview

A photograph of the chamber attached to the LI-6800 head and a CAD schematic of the chamber are given on Figure 1. It is a flush-mount chamber, directly connected to the LI-6800 head via an adapter, allowing the chamber to use the built-in LI-6800 mixing fan, as well as its temperature control[12]. The larger the volume, the longer it takes to reach stable environmental conditions within the chamber for proper measurements. Hence, the dimensions of the chamber were determined to ensure a response time (time constant) of less than 3 minutes with the maximum mass flow rate of the LI-COR 6800, 1400 µmol/s (= 3.41 10^{-5} m^3/s at standard pressure, 101,325 Pa, and average laboratory room temperature, 24°C). A response time of 3 minutes is indeed an acceptable trade-off between the size of the chamber and the time to wait for environmental conditions stabilization between each measurement. The time constant of the chamber τ – defined as the required time to reach about 63% of the desired setpoint – depends on the chamber's volume V and mass flow rate f: $\tau = \frac{V}{f}$.

The chamber's dimensions are 0.15 m (W) x 0.2 m (L) x 0.19 m (H), hence a total volume of 5.70 10^{-3} m^3. Based on the instrument length (0.185 m, so 0.37 m two ways) and the air inlet and outlet diameters (0.015 m), we assume a

tubing volume of 8.33 10^{-5} m^3, hence a total volume of 5.78 10^{-3} m^3 and a time constant of 2 min 49.4 s. The pot used in this chamber has a volume of 1.5 10^{-4} m^3, making the overall usable volume of the chamber smaller, 5.63 10^{-3} m^3, leading to a response time of 2 min 45 s (we neglect the volume of the plant in this calculation). Ultimately, for measurements with a real plant inside the chamber, the soil will be covered to avoid evaporation from the growth media, – which would skew the transpiration measurements.

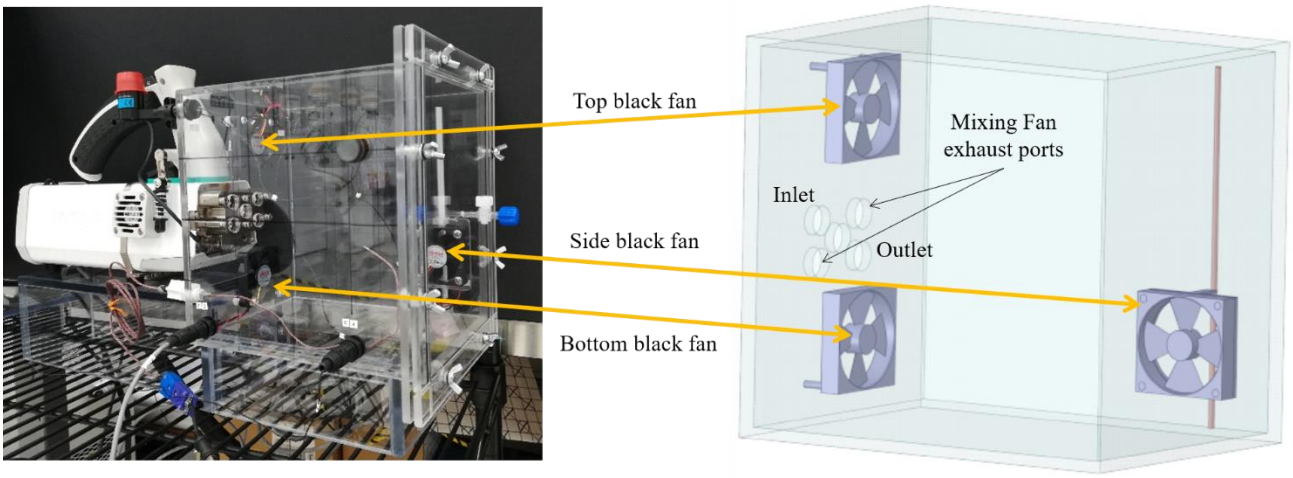

Figure 1. Overview of the LI-6800 custom-made chamber. Left: photograph with LI-6800 attached; one anemometer is attached on the wall facing us (see section II.B. 1); a port in the door enables CO_2 injection for residence time distribution studies (see section II.A); the adapter between the LI-6800 head and the chamber is also shown on the picture. Right: schematic of the chamber displaying the three fans and their respective positions, as well as the LI-6800 attachment ports.

The material used for the chamber's walls is cast acrylic – guaranteeing low rates for adsorption and desorption of water vapor. A material that adsorbs and desorbs water will prevent water vapor from reaching an equilibrium in the chamber[12].

Three extra fans (Akasa, Black Fan, 50 x 10mm, 12v, 3-pin, DFC501012H) are located on the walls of the chamber at different locations, to ensure optimal mixing (see section II.A). Their positioning was determined following preliminary tests on a prototype chamber. Two fans are located above and below the LI-6800 interface and one is on a side wall, with an adjustable height to adapt to different types of plant shapes and canopies.

The chamber is also equipped with a thermocouple that allows leaf temperature measurements and with anemometers that measure airspeed within the chamber (see section II.B).

A. Continuous stirred tank reactor and residence time

The assumption behind the LI-6800 computations is that the chamber is considered as a continuous stirred tank reactor (CSTR)[13], i.e. that at any given time, the air entering the chamber is entirely mixed with the air already there. The residence-time distribution (RTD) was computed for different combinations of fans to characterize the mixing within the chamber and determine the lowest airspeed possibly reachable without violating the CSTR assumption.

1. Methods

An injection port located on the door of the chamber (Figure 1) enabled a pulse input of pure CO_2 – used as our tracer here. Indeed, CO_2 has similar properties as the air within the chamber, does not react with it, and we can easily detect it with the LI-6800. Additionally, it does not adsorb on the walls of the chamber, because they are made of cast acrylic. For each test we measured the concentration of CO_2 within the chamber for 30 min (logging a measurement every 5 s), after injecting 50 mL of pure CO_2 using a syringe, in 1 s (more than 100 times less than the mean residence time). Usually, for residence time measurements, the tracer is injected in the entry port of the reactor, but our set-up did not allow this, so we considered our initial time at the moment when the chamber's concentration in CO_2 was the highest, about 20 s after the injection.

For all tests, the incoming air contained no CO_2 – thanks to the LI-6800 scrubbing system – and had a mass flow of 1400 µmol/s. The temperature and relative humidity were not controlled within the chamber, but were that of the ambient air in the laboratory (23 – 25°C and 50% respectively).

The test was performed on an empty chamber, as well as with an artificial plant and its pot inside the chamber (Figure 2), to account for a plant's volume without having it react with the CO_2 through photosynthesis or respiration.

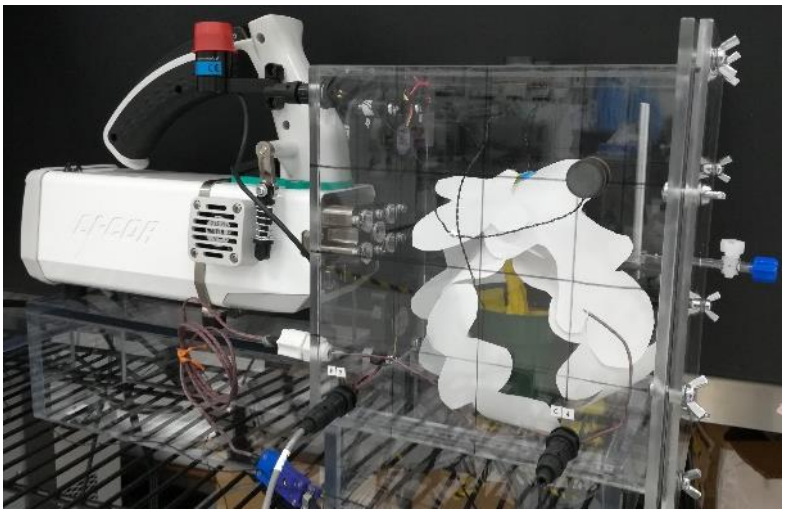

Figure 2. Artificial plant with paper leaves in the custom-made chamber.

The RTD function *E(t)* – concentration function normalized by its integral – gives information on potential dead volumes or bypassing within the chamber:

$$E(t) = \frac{C(t)}{\int_0^\infty C(t)dt}$$

where *C(t)* is the CO_2 concentration function.

The nominal voltage of the black fans is 12 V, but we operate them at lower voltage to maintain lower airspeeds. We checked the linearity of the fans in terms of air velocity output for voltages below 12V. The results are shown in Figure 3, obtained with the anemometer placed centered 3 cm in front of the fan.

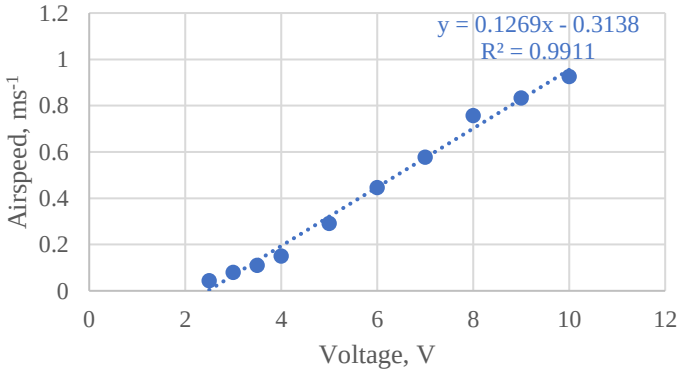

Figure 3. Fan airspeed outputs versus the applied voltage. The fan outputs are linear. This is the output of one fan, representing all three fans.

This allowed us to compute the fans pressure jumps at different voltages, which are proportional to the airflow output at a given voltage. A summary of pressure jumps is given in Table 1; they are used for the CFD computation in part D, as inputs for the fans.

Table 1. Pressure jump of the fans for different voltages.

Voltage (V)	Airflow (dm^3s^{-1})	Pressure Jump (Pa)
12	5.19	1.07
10	4.33	0.74
8	3.46	0.48

6	2.60	0.27
4	1.73	0.12
3.5	1.52	0.09
3	1.30	0.07
2.5	1.08	0.05

Regarding the internal LI-6800 mixing fan, we did not have information about its airflow output, so we measured the velocity at both fan exhausts (top and bottom, see Figure 1) for different RPM values (Figure 4) and deduced the corresponding pressure jump (Figure 5).

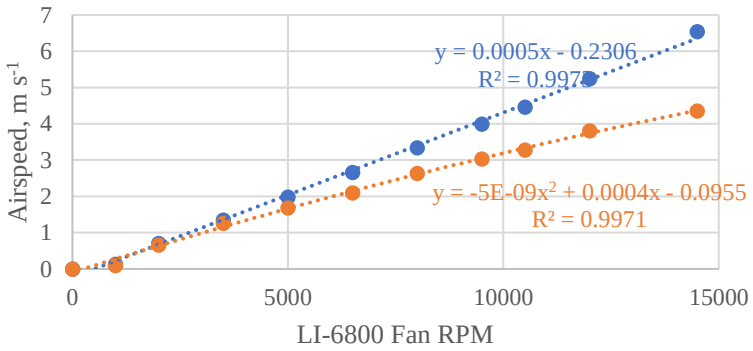

Figure 4. Airspeed at the exhaust of the LI-6800 fan, top (blue dots) and bottom (orange dots) with associated linear trendlines (dotted lines).

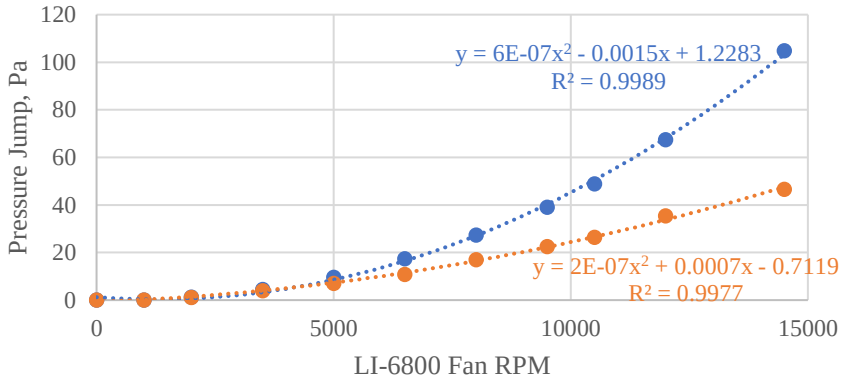

Figure 5. Pressure jump at the exhaust of the LI-6800 fan, top (blue dots) and bottom (orange dots) with associated polynomial trendlines (dotted lines).

Different combinations of fan intensities and positions were tested within the prototype chamber, leading to the final decision of three extra fans in the chamber. In the next paragraph (II.A.2), we present the main results leading to this choice.

2. Results

Two baselines were first established, with and without an artificial plant + pot inside the chamber. For the first baseline, all fans were on at maximum setting; for the second, there was no ventilation from any fan (not even the built-in LI-6800 fan). Results are presented in Figure 7 and Figure 6.

At 24°C, the mean residence time for an ideal CSTR with the volume of the empty chamber is 169.4 s (2 min 49.4 s), while it is 165 s (2 min 45 s) for an ideal CSTR with the volume of the chamber with a plant inside. With no fan, it is 179.7 s in our empty chamber, and 140.4 s in the chamber with the plant. Both values indicate a problem of mixing in the chamber:

- In the first case – empty (Figure 6) – the larger mean residence time is a sign of bypassing, i.e., a fraction of the fluid immediately exits the chamber upon entering: less fluid passes through the system, the volumetric flow rate is thus smaller, leading to a larger residence time. The volume of fluid that bypasses

the chamber, V_b, can be computed, knowing the mean residence time τ_b = 179.7 s, the chamber's volume V = 5.78 10^{-3} m^3, and the volumetric flow rate Q = 3.41 10^{-5} m^3 s^{-1}:

$$V_b = \frac{\tau_b\, Q - V}{\tau_b} = 1.95\ 10^{-6}\ m^3 s^{-1} = 0.057\ Q$$

Hence, 5.7% of the fluid is bypassing the chamber when no fans are set, in an empty chamber.

- In the second case – with artificial plant (Figure 7) – the smaller residence time is a sign of a dead volume in the chamber, i.e., a part of the chamber that the entering fluid does not reach (likely blocked by the plant itself). The dead volume V_{DV} can be computed, using the same notations as previously, but this time with the mean residence time τ_{DV} = 140.4 s:

$$V_{DV} = V - \tau_{DV} Q = 8.40\ 10^{-4}\ m^3 = 0.15\ V$$

Hence, with an artificial plant inside the chamber, 15% of the fluid is a dead volume when no fans are set.

With all fans on at maximum intensity, the mean residence time is 172.8 s in our empty chamber (2 % of bypassing flow rate), and 176 s in the chamber with the plant (6.2 % bypassing flow).

This shows that adding fans enables:

- Removal of the dead volume within the chamber when a plant is present
- Reducing the bypassing in an empty chamber

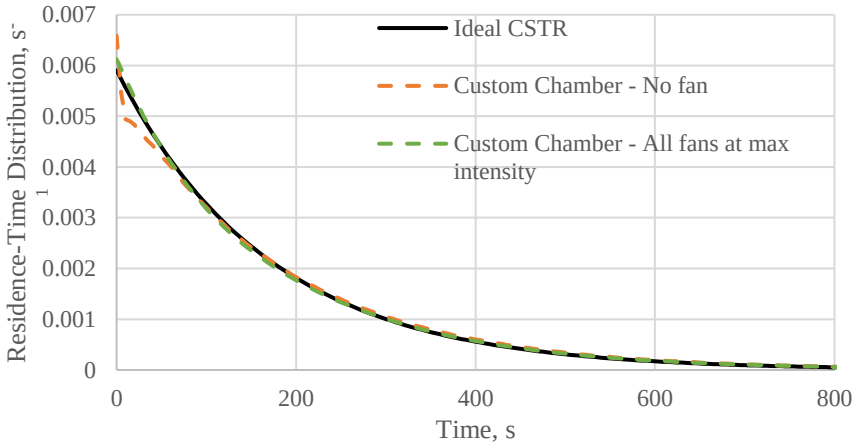

Figure 6. Residence Time Distribution Function for an empty chamber: ideal case of a CSTR (black line), no ventilation (orange dashed line), and with maximum ventilation (green dashed line).

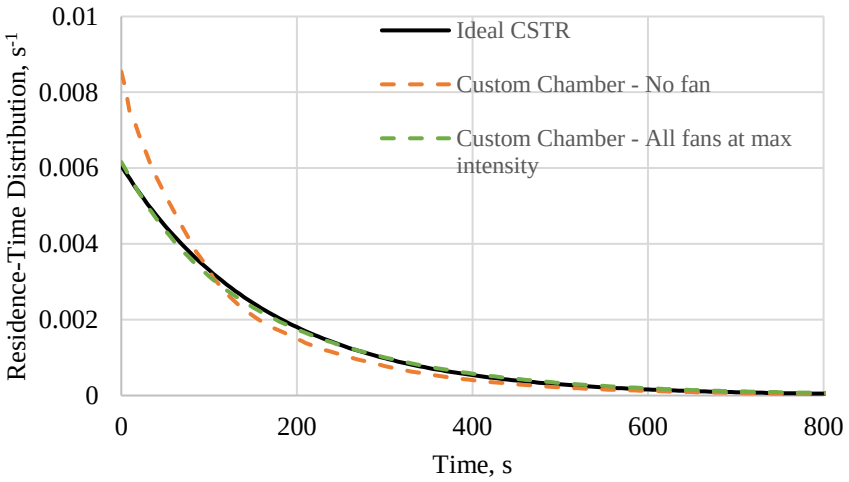

Figure 7. Residence Time Distribution Function for a chamber with an artificial plant inside: ideal case of a CSTR (black line), no ventilation (orange dashed line), and with maximum ventilation (green dashed line).

Because of the configuration of the system, with the inlet close to the outlet, suppressing all bypassing is not possible, but it can be limited and accounted for. Indeed, we can compute the amount of flow bypassing the chamber and correct the flow rate accordingly in our computations of assimilation rate and transpiration. The goal here is to limit it to less than 10%, so that the time constant of the system is not affected too much. For our gas exchange measurements, bypassing is less problematic than a dead volume in the chamber, which means part of the volume would not interact with the reacting system (the plant).

When operated at maximum intensity, the LI-6800 internal mixing fan enables a limited bypassing (4.8%), but the consequence is high airspeed at the leaves' surface. The goal of this custom-made chamber, however, is to perform gas exchange measurements at low airspeed, so this option was not satisfactory, and this fan was not used.

For our application (low airspeed + sufficient mixing), using a combination of two or three fans operated at different voltages seems a good option, providing an adequate mixing while ensuring airspeed lower than 0.1 m/s at the top of the chamber (where the upper leaves will be), as shown in Table 1.

Table 1. Mean Residence Time and Bypassing for different combinations of fan voltages.

Top Fan Voltage (V)	Bottom Fan Voltage (V)	Side Fan Voltage (V)	Mean residence time (s)	Bypassing (%)
2.5	6	0	175.7	6.0
0	6	2.5	177.1	6.8
3	8	0	177.6	7.0
3	4	0	178.5	7.4
0	8	0	179.2	7.9
0	10	0	179.3	8.0
0	0	8	175.9	6.2
0	0	10	175.7	6.0

Raising the voltage of the bottom fan does not significantly increase the air velocity at the top of the chamber, and intuitively, it could be thought as an adequate method for increasing the chamber's mixing. Table 1 shows that this is not the case (rows 3, 5, 6) and that increasing the bottom fan voltage results in a larger percentage of the flow bypassing the chamber. This might be due to the flow bouncing off of the pot and being immediately redirected to the outlet. On the contrary, raising the voltage of the side fan results in reduced bypassing (Table 1, last two rows); it does however increase the airspeed at the top of the chamber (see II.B.2).

Hence, to reach a low velocity in the top of the chamber (<0.1 m/s) without violating the CSTR assumption, the top fan will be operated at 2.5 V and the bottom fan at 6 V. The fan voltage can then be raised to 3 V and 3.5 V to produce higher airspeeds.

B. Airflow map

1. Methods

Four anemometers (CS-9S6SS-A Candlestick sensor, ATS Inc.) were placed in the chamber on magnets, ensuring their mobility within the chamber, in order to measure the airflow at different points; a grid was drawn on the enclosure to facilitate the airflow mapping (Figure 8).

Figure 8. Candlestick anemometer mounted inside the chamber on a magnet and held on the wall of the chamber by another magnet placed outside of the chamber. The grid on the transparent walls can be seen in the background. The diameter of the magnets is 1.8 cm, the length of the candlesticks, 1 cm.

2. Results

3D graphs were generated with the airflow velocity measurements, on the chamber's top and sides, for different fan combinations (Figure 9 and Figure 11). Figure 9 shows that there is a velocity gradient across the chamber, for all combinations except for the maximum voltage one (magenta); the lowest air velocity, compared to the rest of the chamber, appears to be in the corner where the side fan is positioned, close to the door, as shown on Figure 10. This confirms that velocities under 0.1 m/s can be reached at the top of the chamber and that we can make gas exchange measurements with velocities at the leaf surface below 0.1 m/s.

The air velocity on the side walls is uniform for all combinations, except for the maximum voltage scenario (magenta graph, Figure 11). These maps show that on average the air velocity on the side walls is higher than at the chamber's top.

The color code on Figure 9 and Figure 11 are summarized in Table 2.

Table 2. Correspondence between the fan combinations and their colors in the graphs.

Fan combinations	Color
Top fan at 2.5 V and bottom fan at 6 V	Cyan
Bottom fan at 6 V and Side fan positioned mid height at 2.5V	Blue
Bottom fan at 6 V and Side fan positioned low height at 2.5 V	Yellow
Top fan at 2.5 V and Side fan at 3.5 V	Green
All fans at 10 V	Magenta

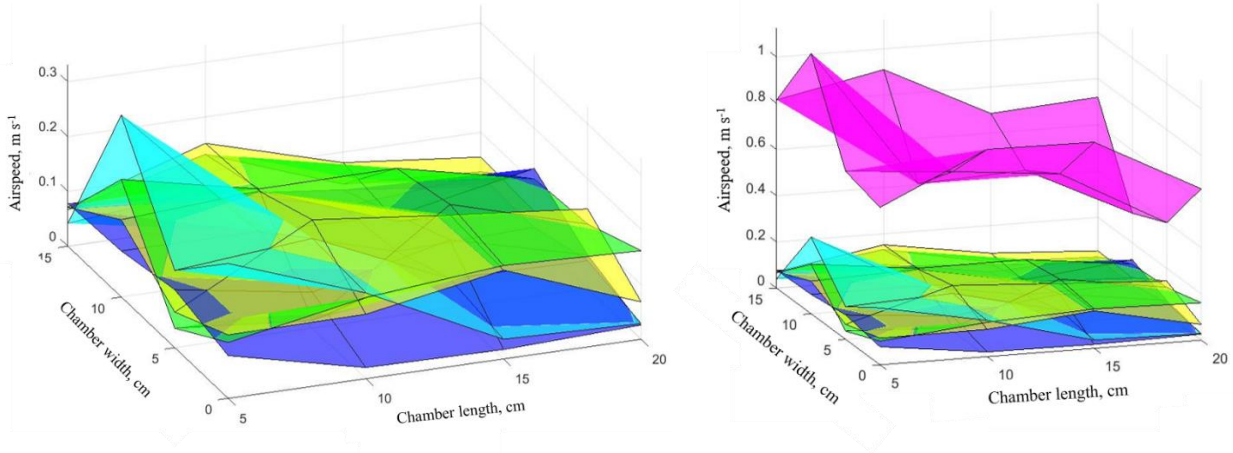

Figure 9. Airflow velocities at the top of the chamber. The top and bottom fan are positioned on the zero of the Chamber Length axis (not shown here). The side fan is positioned between 15 and 20 cm on the Chamber Length axis, at 15 cm on the Chamber Width axis. The graph on the right is the same as the one on the left,

with the addition of the perspective of the maximum velocity (fans at 10 V) compared to the other tests, hence a different scale on the y-axis.

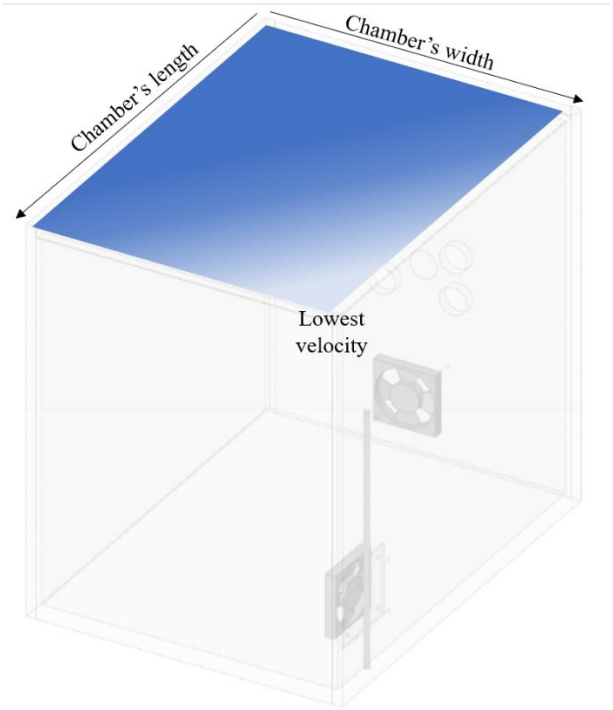

Figure 10. Explanation of chamber's length and width axes. The blue gradient illustrates the velocity gradeint across the top of the chamber.

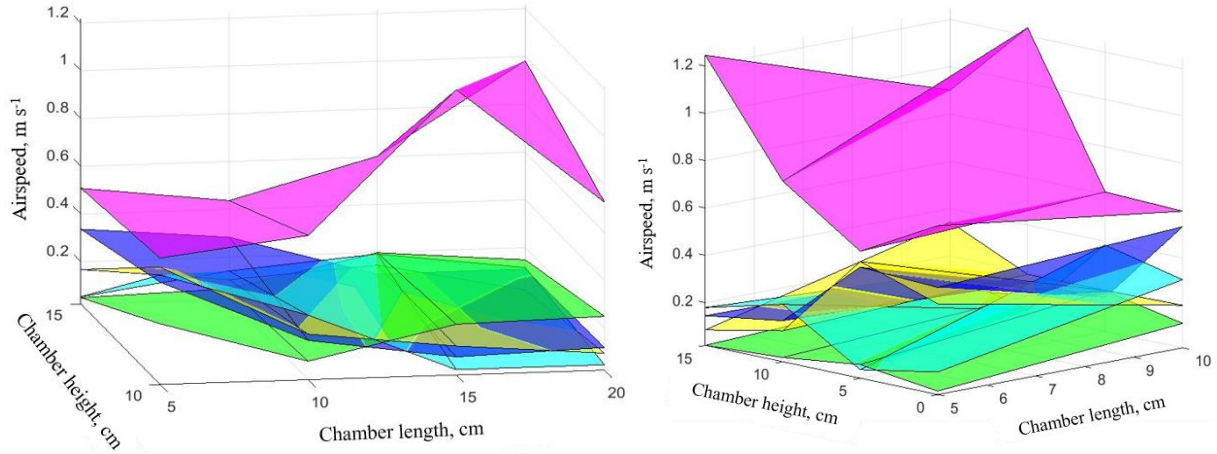

Figure 11. Airflow velocities on the side walls. Left: wall opposite to the one with the side fan (left side when facing the chamber with the LI-6800 in the back). Right: wall hosting the side fan (right side when facing the chamber with the LI-6800 in the back). For the positions of the fans and the color code, see the caption of Figure 9.

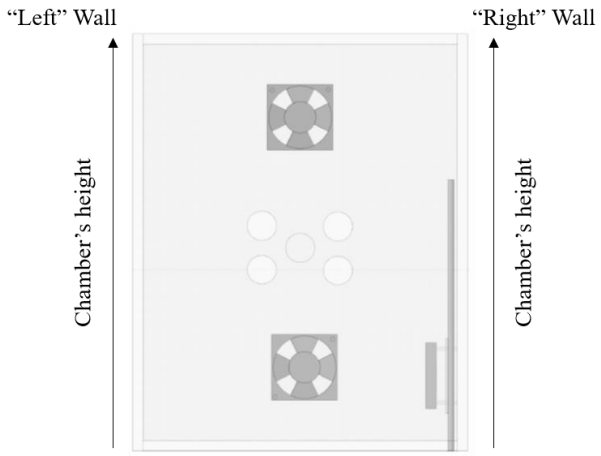

Figure 12. Font view of the chamber with the left and right walls corresponding to the left and right graphs of Figure 11.

III. Computational Fluid Dynamics

A. Methods

The CFD simulations were performed with the commercial software Fluent 19.4.0 for ANSYS 2019 R2. The finite element model is composed of two domains: a fluid region, representing the air within the chamber, and a solid region, representing the plant (Figure 13). The fans (the three extra fans and the LI-6800 built-in fan) are represented as surfaces of same diameter as the fans, that set as fan boundaries, with a defined pressure jump. The LI-6800 fan has two outlets and thus two fan boundaries are set in Fluent to represent them.

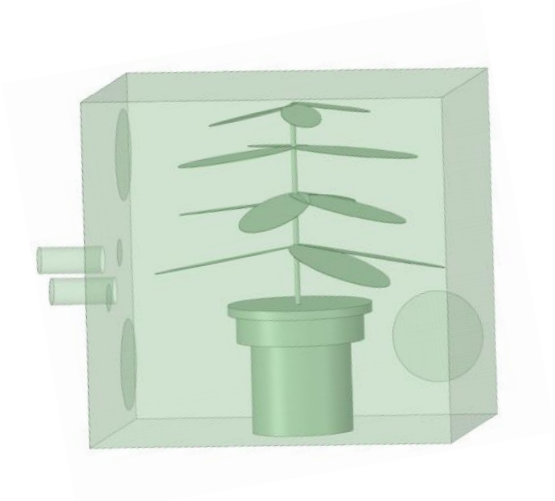

Figure 13. Fluid (air) and solid (plant) regions in Fluent before the CFD simulations. The fans are represented by the circular surfaces within the enclosure.

The mesh is composed of 1,210,988 polyhedral cells, with a maximum skewness of 0.82 and a minimum orthogonal quality of 0.12, which is acceptable.

Given the dimensions of this chamber, the Reynolds number is greater than 2,300 for an airspeed greater than 0.18 m/s. So, the turbulence transition in the chamber happens at 0.18 m/s, which, as we discussed in the previous part, is reached in all combinations of fans, in particular on the walls and edges. Consequently, we used an SST k-omega turbulence model based on the Reynolds Averaged Navier-Stokes Simulation (RANS) equations, applied to the gas domain of the chamber. This is the most basic turbulence model and the one requiring the least computation power. It is sufficient for our application, as the objective of these CFD simulations was to visualize the air path within the

chamber, as well as its velocity, not to detail the turbulence. In fact, the fans are not modeled as rotating wheels, only their effect is modeled.

Three simulations are presented, referred respectively as simulations 1, 2, and 3 hereafter: one where no fan was used, one where only the top and the bottom fans where used, and one where only the top and the side fans were used. In all simulations, the mass flow entering and exiting the chamber (1400 µmol/s), as detailed in section II, is included.

B. Results

Simulation 1 converged after 167 iterations and the side view is given in Figure 14. With no fan, there are many stagnant zones in the chamber (dark blue zones), which is coherent with our findings on the residence time distribution showing 15% of dead volume in the chamber when no fan is used.

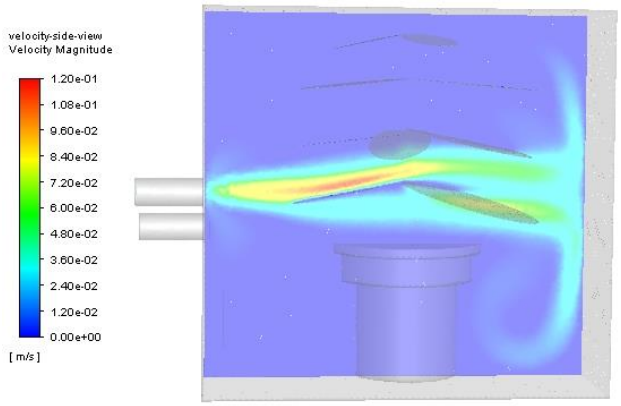

Figure 14. Velocity contour of the air within the chamber (side view) with no fan. The LI-6800 interface is on the left side. Note that the air velocity for simulation 1 is much lower than for the two others. Therefore, to show any effect, the color scale is different.

Simulation 2 was run with the top fan at 2.5 V, corresponding to a pressure jump of 0.046 Pa, and the bottom fan at 6V, corresponding to a pressure jump of 0.27 Pa. The results of this simulation are displayed in Figure 15. The velocity contour (left side) shows that the air pushed by the bottom fan bounces on the pot and circles back to the LI-6800 exhaust. The air velocity in the top of the chamber ranges between 0.03 and 0.15 m/s – like what we found experimentally.

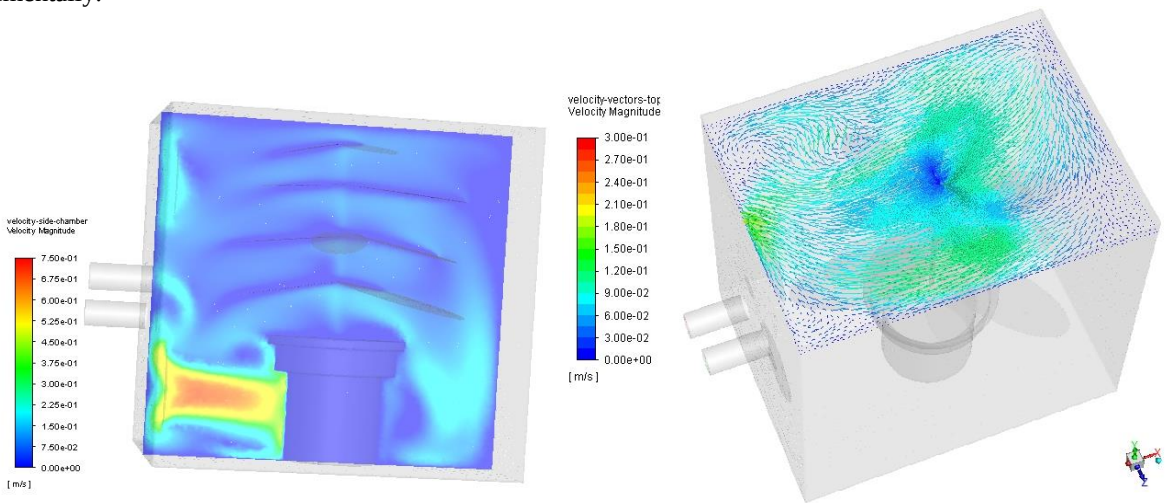

Figure 15. Results of simulation 2. Left: velocity contour of the air within the chamber (side view) with the top fan at 2.5 V and the bottom fan at 6 V. Right: velocity vectors, 1 cm from the chamber's top (top view).

Simulation 3 was run with the side fan at 2.5 V, corresponding to a pressure jump of 0.046 Pa, and the bottom fan at 6 V, corresponding to a pressure jump of 0.27 Pa. The results of this simulation are displayed in Figure 16. The air velocity in the top of the chamber is higher than for simulation 2 – like what we found experimentally.

These simulations also show that, whether or not the side fan is used, the air flow within the chamber has no axial symmetry in its length. This partly comes from the fact that the inlet of the LI-6800 is not centered. Consequently, we will need to account for this when positioning the plant inside the chamber, as well as for gas exchange measurements interpretation.

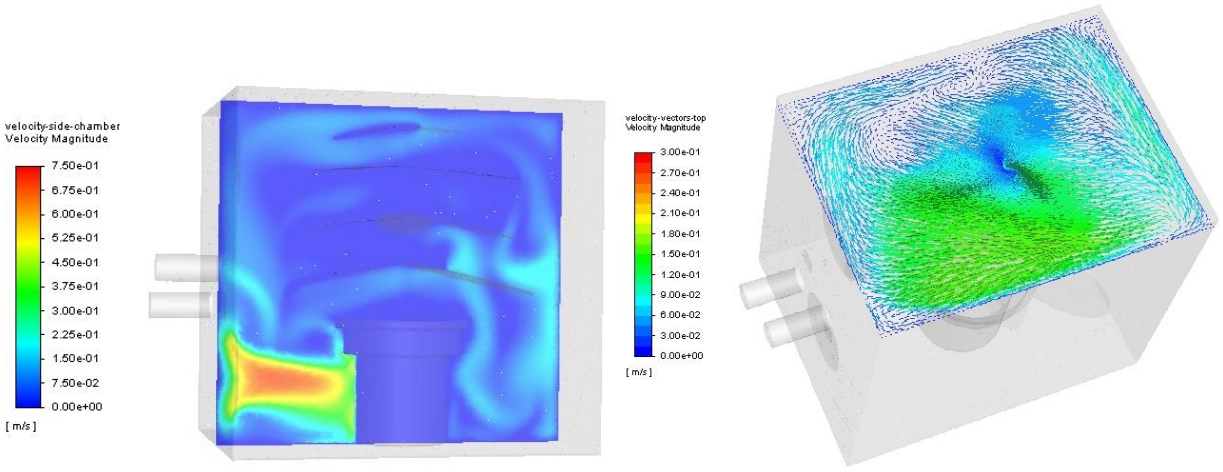

Figure 16. Results of simulation 3. Left: velocity contour of the air within the chamber (side view) with the side fan at 2.5 V and the bottom fan at 6 V. Right: velocity vectors, 1 cm from the chamber's top (top view).

IV. Conclusion and Perspectives

We presented the design and tests of a custom-made chamber that can be interfaced with the LI-6800 for real time photosynthesis measurements of whole plants and small canopies:

- The fans inside the chamber can provide enough mixing so as to not violate the CSTR assumption of the LI-6800 measurements;
- Experimental measurements coupled to CFD simulations have shown that low airspeeds (<0.1 m/s) can be maintained on top of the chamber (where top leaves are located), without compromising the mixing.

This study was performed with an artificial plant – a similar study could be performed with an artificial microgreens canopy to ensure that low airspeeds can be reached at the top of the canopy.

The present CFD model does not include gravity as a parameter and hence does not include natural convection, nor heat exchange. In the future, a more detailed model with these aspects should be developed – natural convection would be present in 1g but not in 0g. Furthermore, the turbulence model could be refined to better reflect fluid dynamics within the chamber.

Lastly, this chamber is made for photosynthesis measurements, so the remaining tests will consist in introducing the reacting system – real plants – inside the chamber. The first species that we will be testing is Daikon radish, as shown in Figure 17. Later, we will test small canopies of microgreens.

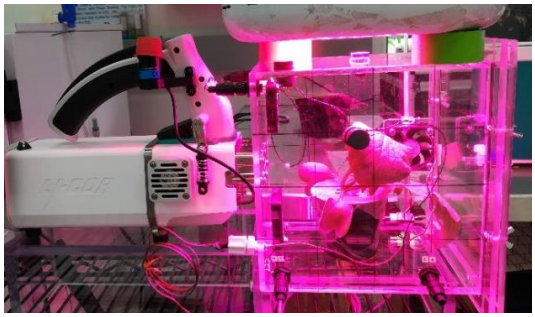

Figure 17. Daikon radish within the custom-made photosynthesis measurement chamber.

Acknowledgments

The authors would like to thank NASA Space Biology through the NASA postdoctoral program / USRA for funding this research.

References

[1]Anderson, M. S., Ewert, M. K., and Keener, J. F., "Life support baseline values and assumptions document", NASA/TP-2015–218570/REV1, 2018.

[2]Wheeler, R. M., "Plants for human life support in space: From Myers to Mars", *Gravitational and Space Biology*, Vol. 23, No. 2, 2010, pp. 26 – 36.

[3]Wheeler, R. M., "Agriculture for space: People and places paving the way", *Open Agriculture*, Vol. 2, No. 1, 2017, pp. 14-32.

[4]Kitaya, Y., Tsuruyama, J., Shibuya, T., Yoshida, M., and Kiyota, M., "Effects of air current speed on gas exchange in plant leaves and plant canopies", *Advances in Space Research*, Vol. 31, No. 1, 2003, pp. 177-182.

[5]Monje O., Stutte, G. W., Goins, G. D., Porterfield, D. M., and Bingham, G. E., "Farming in space: environmental and biophysical concerns", *Advances in Space Research*, Vol. 31, No. 1, 2003, pp. 151-167.

[6]Massa, G. D., Wheeler, R. M., Morrow, R. C., and Levine, H.G., "Growth chambers on the International Space Station for large plants", *Acta Horticulturae*, Vol. 1134, 2016, pp. 215-222

[7]Massa, G. D., Richards, J. T., Spencer, L., Hummerick, M. P., Stutte, G. W., Wheeler, R. M., Douglas, G., and Sirmons, T., "Selection of Leafy Green Vegetable Varieties for a Pick-and-Eat Diet Supplement on ISS", *Proceedings of the 45th International Conference on Environmental Systems*, edited by Texas Tech University Libraries, 2015.

[8]Morrow, R. C., T. M. Crabb, J. R. Iverson, and J. G. Frank, "Science accommodations in the Biomass Production System", *Proceedings of the 31th International Conference on Environmental Systems*, edited by SAE International Technical Paper, 2001.

[9]Kitaya, Y., "Plant factory and space development, Space Farm", *Plant Factory Using Artificial Light: Adapting to Environmental Disruption and Clues to Agricultural Innovation*, edited by M. Anpo, H. Fukuda and T. Wada, 2019, pp. 363-379.

[10]Poulet, L., Fontaine, J.-P., Dussap, C.-G., "A Physical Modeling Approach for Higher Plant Growth in Reduced Gravity Environments", *Astrobiology*, Vol. 18, No. 9, 2018, pp. 1093-1100.

[11]Poulet, L., Dussap, C.-G., Fontaine, J.-P., "Development of a mechanistic model of leaf surface gas exchange coupling mass and energy balances for life-support systems applications", *submitted to Acta Astronautica, in revision*, 2020.

[12]LI-COR, "Using Custom Chambers with the LI-6800", 979-16768, 2017.

[13]LI-COR, "Using the LI-6800 Portable Photosynthesis System", User Manual Version 1.3, 984-15834, 2018.